Magnetic heterostructures with low coercivity for high-performance magneto-optic devices

V A Kotov[1]**, A F Popkov**[2]**, S V Soloviev**[2]**, M Vasiliev**[3]**, K Alameh**[3]**, M Nur-E-Alam**[3] **and D E Balabanov**[1]

[1] Institute of Radio Engineering and Electronics, Russian Academy of Sciences, 11 Mohovaya St, Moscow, 125009, Russia
[2] National Research University of Electronic Technology (MIET), Bld. 5, Pas. 4806, Zelenograd, Moscow, 124498, Russia
[3] Electron Science Research Institute, Edith Cowan University, 270 Joondalup Drive, Joondalup 6027, Australia

E-mail: kotov.slava@gmail.com and m.vasiliev@ecu.edu.au

Abstract
In this work, we analyse the method of forming magneto-optically active heterostructures based on magnetic layers with different magnetic properties. Layers of one type possess a high effective constant of uniaxial magnetic anisotropy K_u^* for which the condition $K_u^* = K_u - 2\pi M_s^2 > 0$ is fulfilled, where K_u is the constant of uniaxial magnetic anisotropy and $2\pi M_s^2$ is the demagnetizing energy, and layers of the second type used possess in-plane or quasi-in-plane magnetization, in which the condition $K_u^* = K_u - 2\pi M_s^2 < 0$ holds true. The layers of the first type, which we refer to as layers of positive effective uniaxial magnetic anisotropy, may have the composition $Bi_2Dy_1Fe_4Ga_1O_{12}$ and the layers of second type the composition $Bi_3Fe_5O_{12}$, which may have very high magneto-optic (MO) figure of merit and are therefore very attractive for the development of MO transparencies and ultra-fast switches. We discuss the optimization of triple-layer structure parameters aimed at achieving a high MO figure of merit simultaneously with low coercivity and high remanent magnetization and possessing rectangular hysteresis loops. The results of the experimental study of the MO properties achieved in garnet heterostructures fabricated using RF sputtering are also described. We show that the proposed paradigm of using new magnetic material combinations demonstrating significantly improved magnetic and MO properties may be realized when working with heterostructures based on Bi-substituted ferrite garnets grown on (1 1 1)-oriented garnet substrates.

(Some figures may appear in colour only in the online journal)

1. Introduction

At present, the main challenge in the field of magneto-optic (MO) materials for use in nanophotonics, integrated optics and broadband communication systems is the development of next-generation nanocomposite-type material systems, which can possess simultaneously a record-high MO figure of merit and high effective uniaxial ($K_u - 2\pi M_s^2 > 0$) magnetic anisotropy sufficient to orient the magnetization of thin films along the normal to the film's plane. The main class of materials used in applied MOs is still represented by Bi-substituted iron garnets of different compositions, since these possess record optical and MO properties in the infrared and visible spectral regions. Thin films of Bi-substituted ferrimagnetic iron garnets obtained using RF-magnetron sputtering or pulsed laser deposition (PLD) are particularly interesting, since these fabrication methods are compatible with the base technologies used in the manufacture of optical integrated circuits.

Of particular interest for applications are multilayer nanocomposite-type structures based on iron garnets suitable

for the next generation of spatial light modulators or MO transparencies providing pixel switching times on the scale of 1–10 ns [1, 2]. A generic transparency-type device can be represented by a matrix composed of a large number of pixels (1024 × 1024) organized in such a way as to enable switching of light transmission or reflection efficiency within arbitrary individual pixels of such a matrix. Currently, various types of transparencies based on liquid crystal materials are available commercially, which possess the characteristic pixel switching response times on the scale of several ms [3]. However, for a number of applications of high practical importance, there is a need for transparencies that possess pixel switching times on the nanosecond scale, which can only be realized if based on using MO or electro-optic materials. Despite a long history of MO transparencies development (some notable works in this field are described in [4, 5]), their fabrication technology has still not been industrialized. A sample of a matrix printer head using MO transparency was manufactured in 1977 [6]. However, for a range of reasons, these printing heads have never been manufactured industrially.

In most cases, the base materials used for making experimental samples of MO transparencies were films of Bi-substituted ferrite garnets possessing positive effective uniaxial magnetic anisotropy, which were grown on monocrystalline garnet substrates using liquid-phase epitaxy (LPE). The substrates used were most often $Gd_3Ga_5O_{12}$ (GGG) or other monocrystalline garnets with lattice parameters exceeding that of GGG. The excellent MO properties of Bi-substituted iron garnets (large specific Faraday rotations) originate from the presence of Bi^{3+} ions within these materials, therefore the garnet of composition $Bi_3Fe_5O_{12}$ should possess the maximum specific Faraday rotation.

Until now, it was not possible to synthesize garnet films of this composition using LPE technology. The maximum Bi content in LPE-grown monocrystalline garnet materials was obtained in $Bi_{2.3}(YLu)_{0.7}Fe_5O_{12}$ [7]. The use of other film growth technologies has led to the successful synthesis of nanocrystalline $Bi_3Fe_5O_{12}$ films by either RF-magnetron sputtering [8] or PLD [9]. Films of various Bi-substituted iron-garnet compositions can be grown using these technologies on practically any substrate type, including glass, silicon and gallium arsenide, with the low growth rates allowing very high accuracy in film thickness control. However, the films with high bismuth content grown using most deposition technologies available generally possess much higher optical absorption across the visible and near-infrared spectral regions (their optical absorption coefficients are usually 3–5 times higher compared with those measured in epitaxially grown garnet films at the same wavelength). As a result, the MO figure of merit ($2\Phi_F/\alpha$) of such MO materials, defined as the doubled ratio of the specific Faraday rotation Φ_F to the optical absorption coefficient α, is normally at levels comparable to the MO figure of merit measured in epitaxial iron-garnet films of composition $Bi_{1.5}Gd_{1.5}Fe_5O_{12}$ grown by LPE.

It was possible to solve the problem of this excess optical absorption by means of modifying the standard technological process of RF-magnetron sputtering [10]. In co-sputtered nanocomposites of bismuth-iron-garnet—bismuth oxide type,
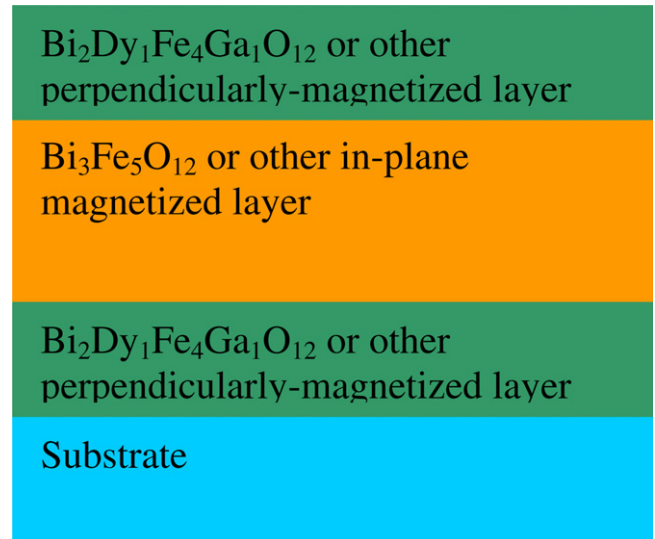

Figure 1. A base block structure of the new functional MO heterostructure-type material system simultaneously possessing high MO performance and high uniaxial magnetic anisotropy ($K_u > 4\pi M_s$), implemented as a triple-layer thin-film structure.

the optical absorption coefficients at 633 nm were measured to be within the range 1000–1200 cm^{-1} [10–12], which corresponds to the lower limit of absorption coefficients achievable in bismuth-substituted iron garnets fabricated using liquid phase epitaxy.

Another important disadvantage of $Bi_3Fe_5O_{12}$ films fabricated using RF-magnetron sputtering or PLD is the absence of growth-induced uniaxial magnetic anisotropy sufficient for orienting the magnetization in the direction perpendicular to the film's plane, i.e. satisfying the condition $K_u > 2\pi M_s^2$. The typical values of the saturation magnetization $4\pi M_s$ in sputtered iron-garnet films, which have been crystallized by post-deposition annealing, are around 1500 Gs. After the annealing treatment, because of the differences in the thermal expansion coefficients between the film and GGG substrate, there appears a small magnetostriction-induced uniaxial magnetic anisotropy K_u^s, but its value is still always smaller than the demagnetization energy density $2\pi M_s^2$.

In this work, we propose to use a triple-layer thin-film structure depicted in figure 1, as a base building block of advanced MO material systems in order to solve the problem of achieving high MO figure of merit simultaneously with high remanent perpendicular magnetization and low coercivity. In such structures, the intermediate layer can be made of MO material possessing record MO properties but also having small uniaxial or even in-plane magnetic anisotropy, such as $Bi_3Fe_5O_{12}$ or other garnet materials. The surrounding layers can be deposited as thin films of materials like $Bi_2Dy_1Fe_4Ga_1O_{12}$ with high effective uniaxial ($K_u - 2\pi M_s^2 > 0$) magnetic anisotropy, but having a smaller specific Faraday rotation. When the thickness of the middle layer is optimized, the magnetization direction of the $Bi_3Fe_5O_{12}$ layer remains close to the film normal. The optimization applied here means that the thickness of the middle layer must be

compatible with the 90° domain wall width existing between the uniaxial ($K_u > 0$) and in-plane ($K_u < 0$) layers.

A MO material system composed of a series of such nanoscale-sized exchange-coupled layers stacked together can ensure larger overall specific Faraday rotation compared with a uniform $Bi_2Dy_1Fe_4Ga_1O_{12}$ film, whilst maintaining the residual perpendicular magnetization direction. As we found later, these composite multilayers can simultaneously possess a rectangular hysteresis loop and rather small values of the coercive force. This result is extremely important for reducing the power dissipation in MO transparencies. Magnetic heterostructures made as double- and triple-layer exchange-coupled films have been studied previously as potential materials for thermo-magnetic information storage in MO discs, but in these applications the criteria used for material system optimization were different from those important for Faraday rotator-type optical devices [13–15]. The aim of this work is to provide a theoretical model and a practical demonstration of a nanocomposite-type high-performance MO material system composed of sequentially deposited nanoscale-sized layers of magnetic materials possessing different uniaxial magnetic anisotropy values.

The material system geometry under consideration includes two uniaxially anisotropic layers with out-of-plane magnetization and one layer with in-plane anisotropy placed in the middle of the structure. Our theoretical description does not include the effects of closure domains on the magnetization behaviour, since we only consider thin magnetic layers of thickness of the order of domain-boundary dimensions, when the domain structure does not appear within uniaxial layers. Experimentally, the effects of domain structure appearance can be observed in thicker layers, and this can lead to measuring somewhat 'tilted' hysteresis loop shapes. Additional theoretical treatment methods are required to consider and predict the domain structure-related effects, which are outside the scope of this work.

The paper is organized as follows: first, we discuss the ways of forming a remanent perpendicularly magnetized heterostructure and the mechanisms of its magnetization according to the theoretical framework relevant to one-dimensional micromagnetic model description. Later, the results of our experimental study of the triple-layer material system based on using two different Bi-substituted garnets deposited by RF sputtering are described. Notable features of magnetic switching behaviour seen in such structures are discussed together with the future development of MO heterostructures possessing controlled values of the MO figure of merit and coercivity.

2. Theory of magnetization behaviour in triple-layer ferromagnetic structures

2.1. Thermodynamic potential of the system under consideration

The magnetization mechanisms of sputtered nanocrystalline heterostructures depend strongly on the character of magnetic domain-boundary localization at the boundaries between
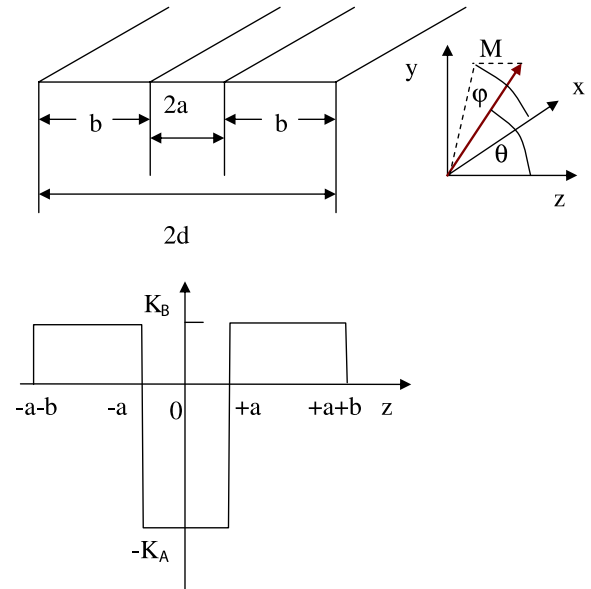

Figure 2. A triple-layer heterostructure (top left) and the coordinate system used (top right). The structure is composed of a middle layer having either small uniaxial or in-plane magnetic anisotropy, where $K_u < 2\pi M_s^2$, surrounded by layers of a high-coercivity material having a high effective uniaxial magnetic anisotropy ($K_u > 2\pi M_s^2$). A modelled dependence of uniaxial anisotropy $K(z)$ on the coordinate along the axis perpendicular to the growth direction of this triple-layer structure is shown below.

nanocrystallite grains, and also on the dispersion of the uniaxial and cubic magnetic anisotropy and on other factors that depend on the technological processes used to form material layers, such as the substrate temperature and annealing regime details. In this section, we focus on the mechanisms of magnetization reversal, induced by the domain wall at the interfaces within the structure. A small magnetic-anisotropy dispersion and strong inter-grain exchange coupling are presumed to exist between the material grains in nanocrystalline layers, as well as either the absence of domain structure or the existence of fixed-location domains in the structure's plane (for example, at the grain boundaries). The possible influence of these factors on the magnetic hysteresis behaviour and the stability of uniformly magnetized state will be discussed later in the experimental section.

Let us consider a triple-layer magnetic heterostructure, as shown in figure 2, which is composed of two layers of thickness b, each having its direction of the easy magnetization axis perpendicular to the layer's plane (z-axis), and an intermediate layer of thickness $2a$ having in-plane magnetization. Furthermore, we will assume that the growth direction of the heterostructure's layers coincides with the [1 1 1] axis of their cubic-lattice ferromagnetic structure. We shall also suppose that in parallel with the uniaxial stress-induced magnetic anisotropy caused by the lattice mismatch there also exists magneto-crystalline cubic anisotropy.

The thermodynamic potential of a ferromagnetic material with combined magnetic anisotropy having the symmetry type of a rhombohedral crystal, and in a set of basis vectors $\tilde{e}_x = (1/\sqrt{2})(1, -1, 0)$, $\tilde{e}_y = (1/\sqrt{6})(1, 1-2)$,

$\tilde{e}_z = (1/\sqrt{3})(1, 1, 1)$, can be represented in the form

$$F = A[(\nabla_z m_x)^2 + (\nabla_z m_y)^2 + (\nabla_z m_z)^2] + K(z)m_z^2 + K^{(1)}m_z^4$$
$$+ K^{(2)}m_y m_z(3m_x^2 - m_y^2) - \boldsymbol{HM},$$

where $m_{x,y,z}$ are the components of the unit magnetization vector $\boldsymbol{m} = \boldsymbol{M}/M$ within layers, A is the exchange stiffness parameter, $K^{(i)}$ are the fourth-order anisotropy constants connected with the cubic crystalline magnetic anisotropy, and the second-order effective magnetic anisotropy $K(z)$ varies across the structure, as shown in figure 2. After taking into account the demagnetization energy $2\pi M_s^2$, the effective anisotropy parameters of second order for the cubic crystal with the magneto-crystalline anisotropy parameter K_1 and induced uniaxial anisotropy $K_U^{A(B)}$ in the corresponding magnetic layer may be presented as $K_A = -K_U^A + 2\pi M^2 + K_1/2 > 0$ for layer A with 'in-plane' anisotropy, and as $K_B = K_U^B - 2\pi M^2 - K_1/2 > 0$ for layers B with perpendicular to the film plane easy magnetization axis, which is parallel to the z-axis. Other anisotropy parameters can be expressed using the cubic anisotropy constant as follows: $K^{(1)} = (7/12)K_1$, and $K^{(2)} = -(\sqrt{2}/3)K_1$. In polar coordinates, where z is used as the polar axis, and the azimuth angles are counted starting from the x-axis, the free energy density can be represented as

$$F = A\left(\left(\frac{d\theta}{dz}\right)^2 + \left(\frac{d\varphi}{dz}\right)^2 \sin^2\theta\right) - K(z)\cos^2\theta$$
$$+ K^{(1)}\cos^4\theta + K^{(2)}\sin^3\theta\cos\theta\sin 3\varphi$$
$$- H_x M\sin\theta\cos\varphi - H_y M\sin\theta\sin\varphi - H_z M\cos\theta, \quad (1)$$

The thermodynamic potential (1) will be used below to seek micromagnetic stationary states in the multilayer structure and to analyse their stability by solving the Landau–Lifshitz equations.

2.2. Uniform magnetization condition of the three-layer magnetic heterostructure

Landau–Lifshitz variational dynamics equations have the form

$$\frac{\partial\theta}{\partial t} = -\frac{\gamma}{M}\frac{F_\varphi}{\sin\theta}, \quad (2)$$

$$\frac{\partial\varphi}{\partial t}\sin\theta = \frac{\gamma}{M}F_\theta, \quad (3)$$

where M is the magnetization, and γ is the magneto-mechanical ratio. The stationary magnetization states of the structure satisfy the condition $F_\theta = F_\varphi = 0$. In the absence of a magnetic field (when $\boldsymbol{H} = 0$), the partial solution that satisfies the equilibrium conditions is represented by the uniform magnetization states $\theta = 0$, or $\theta = \pi$ for an arbitrary azimuthal angle φ.

Let us now consider the conditions for stability of these states. To simplify the analysis, we treat the parameters A, $K_\perp$, M, γ as being identical in all layers, thus implying that the influence of spatial changes in uniaxial anisotropy $K(z)$ is most significant. Let us consider spin deviations near a uniformly magnetized equilibrium state $\theta_0 = 0$, restricted by the condition $\theta \ll \pi/2$. Then it follows from equation (2) that

in the linear approximation at the limit of $\theta(z, t) \to 0$, we have $\partial\theta/\partial t = 0$, so that the deviation of the magnetization vector in the polar angle θ is not time-dependent, and is dependent only on the spatial coordinate z. Equation (3) then defines the structure of soft mode $\theta = \theta(z)$ of the transition as well as the spin precession frequency $\partial\varphi/\partial t = \omega$ of the magnetization around the z-axis. By linearizing this equation, we get

$$\frac{2\gamma}{M}\left(-A\frac{\partial^2\theta}{\partial z^2} + K(z)\theta\right) = \omega\theta. \quad (4)$$

At interfaces of the structure, when $|z| = a$, the continuity of angle θ and of its spatial derivative must be obeyed:

$$\theta(a - 0) = \theta(a + 0), \qquad \left.\frac{\partial(\theta)}{\partial z}\right|_{(a-0)} = \left.\frac{\partial(\theta)}{\partial z}\right|_{(a+0)}. \quad (5)$$

At the external boundaries of the structure, when $|z| = d = a + b$, we suppose the absence of spin pinning, i.e. we apply the free spin condition

$$\left.\frac{\partial(\theta)}{\partial x}\right|_{|z|=d} = 0. \quad (6)$$

We also note that similar conditions also apply for a periodic structure of the period $\Lambda = 2d$. Because of symmetry conditions, the lower frequency branch of oscillations will correspond to an even mode, for the analysis of which it is sufficient to consider only the interval $0 < z < d$. Then, at the left boundary of this interval at $x = 0$, the boundary condition has the form

$$\left.\frac{\partial(\theta)}{\partial x}\right|_{z=0} = 0. \quad (7)$$

Therefore, equation (4) with the boundary conditions (5)–(7) at the interval $0 < z < d$ represents a Sturm–Liouville eigenvalue problem for the oscillation frequency. The stability of homogeneous state $\theta_0 = 0$ is breached when the oscillation frequency tends to zero, when $\omega = 0$. In this case, it follows from equation (4) that the structure of oscillation mode can be described by

$$A\frac{\partial^2\theta}{\partial z^2} - K(z)\theta = 0. \quad (8)$$

In this case, near the equilibrium state $\theta = 0$ there exists degeneracy of unstable modes, i.e. the value of azimuthal angle φ is undefined, and in the linear approximation the directional change is allowed in an arbitrary direction for the unstable mode. The absence of any unambiguous choice of the transition mode is related to the disappearance of basis anisotropy in the linear approximation when $\theta \to 0$. Accounting for the terms of the thermodynamic potential (1) that are non-linear in θ leads to the dependence of thermodynamic potential on the azimuth angle φ, and then the selection of the unstable transition mode becomes unambiguous. Thus, when $\theta > 0$, the preferred angles of magnetization orientation change in the case when $K_1 > 0$ are

$$\varphi_n = \pi/6 + 2\pi n/3, n = 0, 1, 2\ldots. \quad (9)$$

The solution of non-autonomous equation (8) has the form

within interval $0 < z < a$　　　$\theta = \theta_0 \cos(z/\sqrt{A/K_A})$,

$$(10)$$

and

within interval $a < z < d$

$$\theta = \theta_1 \cosh(z/\sqrt{A/K_B}) + \theta_2 \sinh(z/\sqrt{A/K_B}), \quad (11)$$

where θ_0, θ_1, θ_2 are the integration constants. Within interval $0 < z < a$, the odd term is omitted because of symmetry conditions. Taking the boundary conditions (5)–(7) into account leads to a system of algebraic equations for the constants θ_0, θ_1, θ_2:

$$\begin{pmatrix} -\cos(a/\sqrt{A/K_A}) & \cosh(a/\sqrt{A/K_B}) \\ (\sqrt{K_A/K_B})\sin(a/\sqrt{A/K_A}) & \sinh(a/\sqrt{A/K_B}) \\ 0 & \sinh(d/\sqrt{A/K_B}) \end{pmatrix}$$

$$\begin{pmatrix} \sinh(a/\sqrt{A/K_B}) \\ \cosh(a/\sqrt{A/K_B}) \\ \cosh(d/\sqrt{A/K_B}) \end{pmatrix} \begin{pmatrix} \theta_0 \\ \theta_1 \\ \theta_2 \end{pmatrix} = 0. \quad (12)$$

The condition of non-trivial solution existence for this system imposes limitations on the magnetic and geometric parameters of the structure being considered, in particular, the critical thickness of the in-plane magnetized layer for the mode under consideration is defined by

$$b_c = \frac{\sqrt{A/K_B}}{2} \ln \frac{1 + \sqrt{K_A/K_B}\tan(a/\sqrt{A/K_A})}{1 - \sqrt{K_A/K_B}\tan(a/\sqrt{A/K_A})}. \quad (13)$$

It follows from equation (13) that there exists a condition $\sqrt{K_A/K_B}\tan(a/\sqrt{A/K_A}) \geqslant 1$, when the uniform magnetization state becomes unstable with respect to the mode under consideration for any arbitrary thickness of the outer layers with high effective uniaxial magnetic anisotropy. In this case, inside the layer with the in-plane easy axis, a domain boundary will appear. In this case, the appearance of domain wall inside the 'in-plane' layer takes place. In the opposite case, when $\sqrt{K_A/K_B}\tan(a/\sqrt{A/K_A}) < 1$, the appearance of a uniformly magnetized state $\varphi = 0$, $\theta = \pi/2$ is possible, if the thickness of the layer with high effective uniaxial magnetic anisotropy exceeds the critical width (13). The analysis of thermodynamic potential (1) averaged over the thickness of the structure's layers $\langle F(\theta_0) \rangle = (1/(a+b)) \int_0^{a+b} F(\theta(z)) \, \mathrm{d}z$ for infinitesimally small values of cubic anisotropy $K_1 \ll K_A$, in the vicinity of the critical values of thickness $b = b_c(a)$, shows that increases in the amplitude $\theta_0 > 0$ (for the soft mode of the transition (10)–(11) under consideration), with the variations in the structure thickness or anisotropy near their critical values, are continuous. Therefore, the transition towards a non-uniform state $\theta = 0$, $\varphi = \varphi_n$ is a phase transition of the second kind.

Let us consider the asymptotic behaviour of equation (13). When $\sqrt{K_A/K_B}\tan(a/\sqrt{A/K_A}) \to 1$, we have $b_c \to \infty$. This means that the thickness of the layer with in-plane magnetic anisotropy (middle layer of the structure under consideration) should not exceed three times the thickness of the domain boundary, i.e. $2a < \pi\sqrt{A/K_B}$. When $\sqrt{K_A/K_B}\tan(a/\sqrt{A/K_A}) \ll 1$, we have $b_c \approx (\sqrt{AK_A}/K_B)\tan(a/\sqrt{A/K_A})$, i.e. the thickness of the
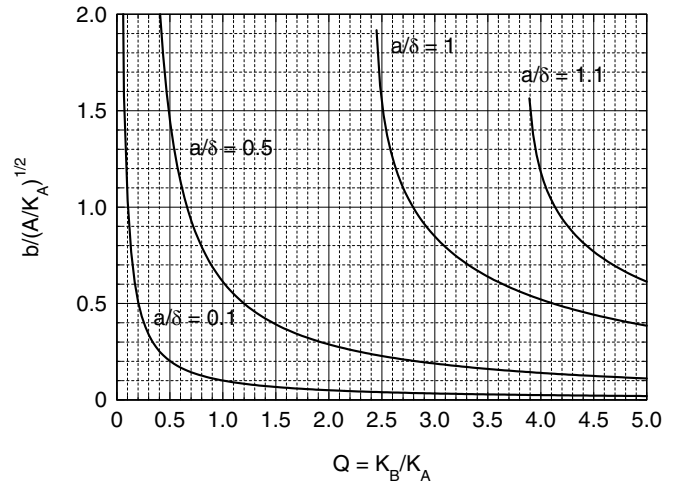

Figure 3. Dependence of the normalized critical thickness of the layer with the positive effective anisotropy $K_B = K_U^B - 2\pi M^2 - K_1/2 > 0$ on the ratio of effective anisotropy parameters of layers $Q = K_A/K_B$.
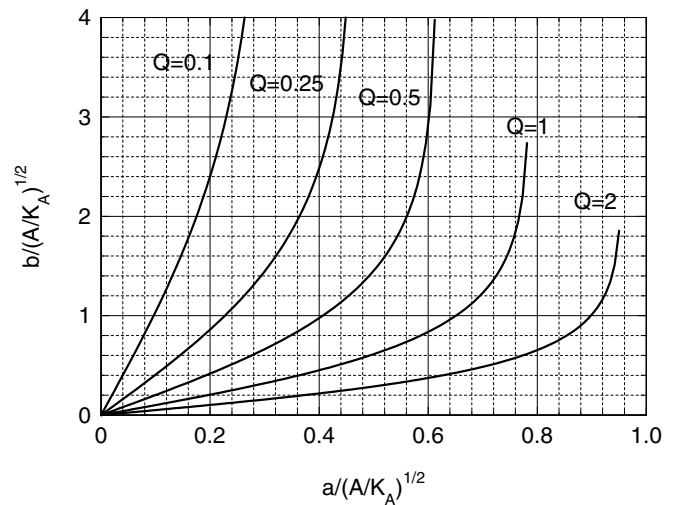

Figure 4. Dependence of normalized critical thickness of the layer with $K_B = K_U^B - 2\pi M^2 - K_1/2 > 0$ on the normalized thickness of the in-plane magnetization layer in which $K_A = -K_U^A + 2\pi M^2 + K_1/2 > 0$.

layer with high effective uniaxial magnetic anisotropy should exceed the domain-wall thickness. For very thin layers, when $b, a \ll \sqrt{A/K_A}$, $\sqrt{A/K_B}$, the obtained condition of uniform magnetization is realized when the thicknesses of the high effective uniaxial magnetic anisotropy layers and the 'in-plane' (middle) layer are related to each other as their anisotropy ratio, i.e. $b/a \approx K_A/K_B$. The latter condition corresponds to the energy equality of the in-plane and out-of-plane component contributions of the structure's layers.

Figure 3 shows the dependence of critical thickness $b_c(Q)$ on the anisotropy energy ratio of the layers $Q = K_B/K_A$, calculated using equation (13) for several values of in-plane layer thickness a, normalized by the domain-boundary thickness $\delta = \sqrt{A/K_A}$. Figure 4 shows the dependence of critical thickness of the layer $b_c(a)$ with high effective uniaxial magnetic anisotropy ($K_u > 2\pi M_s^2$), on the

thickness a of the layer having an in-plane magnetic anisotropy, for different values of parameter $Q = K_B/K_A$.

2.3. Magnetization-reversal field of three-layer heterostructures

The magnetization-reversal process within the triple-layer structure of figure 2 depends on the inter-relationships of the layer thicknesses and anisotropy parameters. In the limit of zero thickness of the intermediate layer, when it is much smaller than the domain-wall thickness, the structure's magnetization-reversal field is close to the effective uniaxial anisotropy field $H_k^* = H_k - 4\pi M_s^2$ of the anisotropy field of outer layers, which maintain the uniform magnetization. Increasing the intermediate layer thickness leads to a rapid reduction in the magnetization-reversal field due to the formation of a domain wall within the layer, which serves as the nuclei of magnetization reversal process [16]. It is also possible to extend the analysis shown above whilst accounting for the effect of external magnetic field. Let us discuss the coercive force in the framework of the spatially non-uniform magnetization switching model described using the thermodynamic potential (1) when the following conditions are applied: $K_1 = K_2 = 0$, $\mathbf{H} = (0, 0, H)$, and the plane of magnetization reversal is fixed at $\varphi = \pi/2$. Then,

$$F = A\left(\frac{\mathrm{d}\theta}{\mathrm{d}z}\right)^2 - K(z)\cos^2\theta - HM\cos\theta, \qquad (14)$$

where $K(z) = -K_A$ for $z < 0$, and $K(z) = K_B$ for $z > 0$ (as shown in the figure below).

Here, the effective anisotropy parameters account for the contributions of both the demagnetization energy and the uniaxial anisotropy, so that $K_A = -K_U^A + 2\pi M^2 > 0$.

The process of non-uniform magnetization reversal in layers with the thickness significantly exceeding the corresponding domain-wall thickness can easily be analysed in the limit of two semi-infinite layers. Calculations show that, in this case, domain wall localized at the interface ceases to exist there, and its width tends to infinity, when the critical value of the angle $\theta_0 = \pi/2$ is reached at the interface (if the layer magnetizations are different, this critical angle depends on the relationship between the magnetic parameters of layers). For $K_B/K_A < 3$, the critical value of the magnetization reversal field is defined by the formula

$$H_c = \frac{2K_B/M}{\sqrt{1 + K_B/K_A} + 1}. \qquad (15)$$

In the opposite case, i.e. when $K_B/K_A > 3$,

$$H_c = \frac{K_A + K_B}{2M}. \qquad (16)$$

For a finite thickness of heterostructure's layers, the solutions of equation (2) are analysed numerically. The calculated dependence of the magnetization-reversal field H_c for a hypothetical triple-layer structure $Bi_2Dy_1Fe_4Ga_1O_{12}/Bi_3Fe_5O_{12}/Bi_2Dy_1Fe_4Ga_1O_{12}$ on the intermediate layer thickness a for different thicknesses b of the layers with $K_U^B > 2\pi M^2$ is
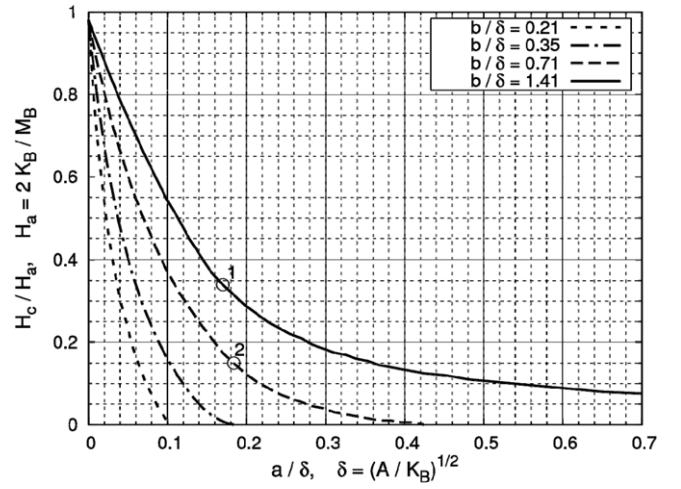

Figure 5. Dependence of the critical magnetization-reversal field for a hypothetical triple-layer structure $Bi_2Dy_1Fe_4Ga_1O_{12}/Bi_3Fe_5O_{12}/Bi_2Dy_1Fe_4Ga_1O_{12}$ on the thickness of the intermediate layer having the in-plane magnetic anisotropy $K_A = -K_U^A + 2\pi M^2 > 0$. The coercive field H_c is normalized by the effective anisotropy field of the uniaxial layer $H_a = 2K_B/M_s = 750$ Oe. All thicknesses are normalized by the domain-wall thickness $\delta = \sqrt{A/K_B} = 58$ nm of the uniaxial layer having $K_B = K_U^B - 2\pi M^2 > 0$. Points 1 and 2 show the critical values of thickness of the in-plane anisotropy layer, above which the hysteresis loop shape is no longer rectangular.

shown in figure 5. The structure's parameters were chosen as follows: for the high effective uniaxial magnetic anisotropy layer $Bi_2Dy_1Fe_4Ga_1O_{12}$ having $K_U^B > 2\pi M^2$ we specify $4\pi M_s = 300$ Gs, $K_u = 0.9 \times 10^4$ erg cm^{-3}, and for the internal $Bi_3Fe_5O_{12}$ layer we use values of $4\pi M_s = 1500$ Gs, and $K_u = 1.8 \times 10^4$ erg cm^{-3}.

Changes in the thickness of the layer with easy in-plane magnetization $K_A = -K_U^A + 2\pi M^2 > 0$ near the critical value lead to the transition from a square hysteresis loop (characterized by a strong perpendicular magnetization in the absence of an external field), towards an inclined hysteresis loop with a reduced remanent magnetization because of the appearance of non-uniform magnetization distribution across the structure's thickness, as can be seen from the comparison of magnetic hysteresis loops shown in figure 6. It follows from the results presented that the effective anisotropy reduction in the relatively thick intermediate layer towards zero allows realization of a uniform magnetization state in this layer. It is because of the coupling with the high-coercivity layers, the thickness of which exceeds their domain wall width. In reality, the in-plane film (middle layer) has usually a rather high coercive force near 100 Oe. The magnetization-reversal field in triple-layer structures with arbitrarily thick outer layers can be reduced by up to three quarters of its value within individual layers. In structures with a finite high-coercivity layer thickness, the coercivity of the heterostructure can be reduced almost to zero with the increasing thickness of the intermediate layer. However, in real epitaxial iron-garnet structures there will always remain a natural cubic lattice-induced anisotropy energy, which can increase the remanent magnetization, on the one hand, and on the other hand, it places
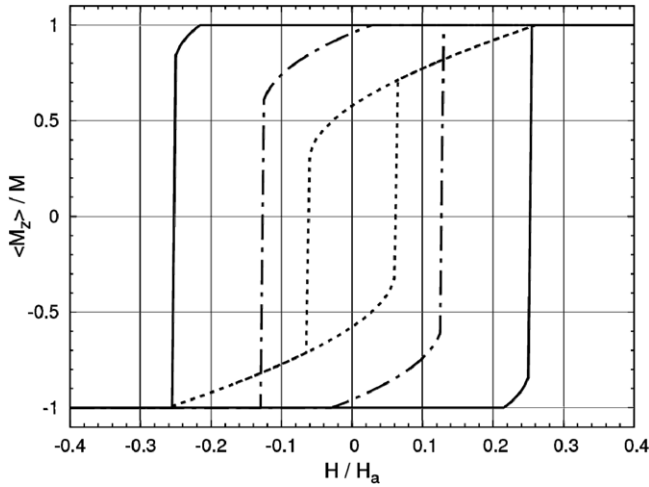
J. Phys. D: Appl. Phys. **46** (2013) 035001

V A Kotov *et al*

Figure 6. Magnetic hysteresis loop of a hypothetical triple-layer structure $Bi_2Dy_1Fe_4Ga_1O_{12}/Bi_3Fe_5O_{12}/Bi_2Dy_1Fe_4Ga_1O_{12}$ for different thicknesses of the in-plane magnetization layer: (*a*) normalized layer thickness is $a/\delta = 0.23$ (continuous line); (*b*) $a/\delta = 0.42$ (dashed line); (*c*) $a/\delta = 1.06$ (dotted–dashed line). The rest of the calculation parameters are described within the text.

a lower limit (being the cubic anisotropy field value) on the magnetization-reversal field.

Moreover, in real structures fabricated by RF sputtering, the polycrystalline texture also leads to additional peculiarities of the magnetization-reversal process related to the anisotropy dispersion in polycrystalline layers.

It is notable that the results shown above can easily be generalized for the case of step-wise changes in the parameters such as magnetization $M(z)$ and anisotropy $K_i(z)$ analogous to the uniaxial anisotropy $K(z)$ changes within the structure's layers. This follows from the fact that the critical thickness b_c of the high effective uniaxial magnetic anisotropy layer depends only on the effective anisotropy parameters K_i and the domain-boundary thickness $\sqrt{A/K_i}$ in each layer with its corresponding direction of magnetization reversal.

3. Experimental study of triple-layer all-garnet heterostructures

It can therefore be expected that some progress in the creation of composite-type MO heterostructures can be achieved in terms of obtaining improved MO figures of merit together with reduced coercivity and high remanent magnetization, by way of sequencing layers with easy in-plane and out-of-plane magnetization axes. We fabricated garnet films of compositions $Bi_2Dy_1Fe_4Ga_1O_{12}$, $Bi_2Dy_1Fe_{4.3}Ga_{0.7}O_{12}$ and $Bi_{1.8}Lu_{1.2}Fe_{3.6}Al_{1.4}O_{12}$ using RF-magnetron sputtering. The films were deposited onto substrates heated up to 250 °C, and all films were initially amorphous (no MO effects were observed) after the deposition. The films were then annealed in air atmosphere at temperatures ranging between 600 and 680 °C, and the annealing process durations varied between 30 min and 12 h.

After running the annealing processes, the film samples were studied magnetically (by measuring their hysteresis loops and Curie temperatures), optically (by measuring the
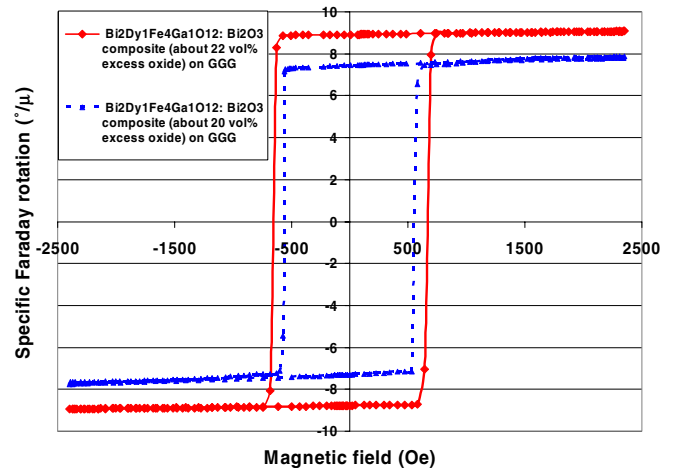

Figure 7. Results of magnetic hysteresis loop measurements obtained on nanocomposite bismuth-substituted iron–garnet–bismuth oxide films of composition type $Bi_2Dy_1Fe_4Ga_1O_{12} : Bi_2O_3$ obtained by co-sputtering of $Bi_2Dy_1Fe_4Ga_1O_{12}$ and Bi_2O_3 targets [17, 18].

absorption spectra between 300 and 2500 nm) and magneto-optically by measuring their specific Faraday rotation spectra between 350 and 900 nm, and also magnetic circular dichroism (MCD) spectra between 280 and 800 nm. In films of composition $Bi_{1.8}Lu_{1.2}Fe_{3.6}Al_{1.4}O_{12}$ the magnetization in the demagnetized state was practically in the film's plane, and in films of $Bi_2Dy_1Fe_4Ga_1O_{12}$ and $Bi_2Dy_1Fe_{4.3}Ga_{0.7}O_{12}$ the remanent magnetization was oriented along the normal to the film's plane after applying saturated magnetic fields between 1 and 2 kOe. The hysteresis loops of the films of composition $Bi_2Dy_1Fe_4Ga_1O_{12}$ and $Bi_2Dy_1Fe_{4.3}Ga_{0.7}O_{12}$ were close to rectangular in shape, and their coercive force values were between 0.6 and 1.2 kOe (figure 7).

We also fabricated single-layer films of composition $Bi_{1.8}Lu_{1.2}Fe_{3.6}Al_{1.4}O_{12}$ and single-layer nanocomposite films of composition type $Bi_{1.8}Lu_{1.2}Fe_{3.6}Al_{1.4}O_{12} : Bi_2O_3$. The films of $Bi_{1.8}Lu_{1.2}Fe_{3.6}Al_{1.4}O_{12}$ were post-deposition annealed at 650 °C, whilst the nanocomposite films $Bi_{1.8}Lu_{1.2}Fe_{3.6}Al_{1.4}O_{12} : Bi_2O_3$ were crystallized at 580 °C. MO measurements showed that after the annealing crystallization, these films possessed quasi-in-plane anisotropy (their magnetization vector direction was inclined at a small angle with respect to the film's plane), since we used (1 1 1)-oriented gadolinium gallium garnet (GGG) substrates. The coercive force value measured in the $Bi_{1.8}Lu_{1.2}Fe_{3.6}Al_{1.4}O_{12}$ films was about 50 Oe, and about 30 Oe in the nanocomposite films of type $Bi_{1.8}Lu_{1.2}Fe_{3.6}Al_{1.4}O_{12} : Bi_2O_3$. The results of hysteresis loop measurement are shown in figure 8.

We manufactured a triple-layer sample of an all-garnet heterostructure, the outer layers of which were of composition $Bi_2Dy_1Fe_4Ga_1O_{12}$ and its intermediate layer was $Bi_{1.8}Lu_{1.2}Fe_{3.6}Al_{1.4}O_{12}$. The structure was deposited using RF-magnetron sputtering onto a GGG (1 1 1) substrate, and its magnetic and MO properties were studied. The samples of this all-garnet triple-layer structure were crystallized by annealing at 570 °C, and demonstrated a rectangle-like magnetic hysteresis loop with coercivity of nearly 90 Oe when reversing the magnetization direction in external fields
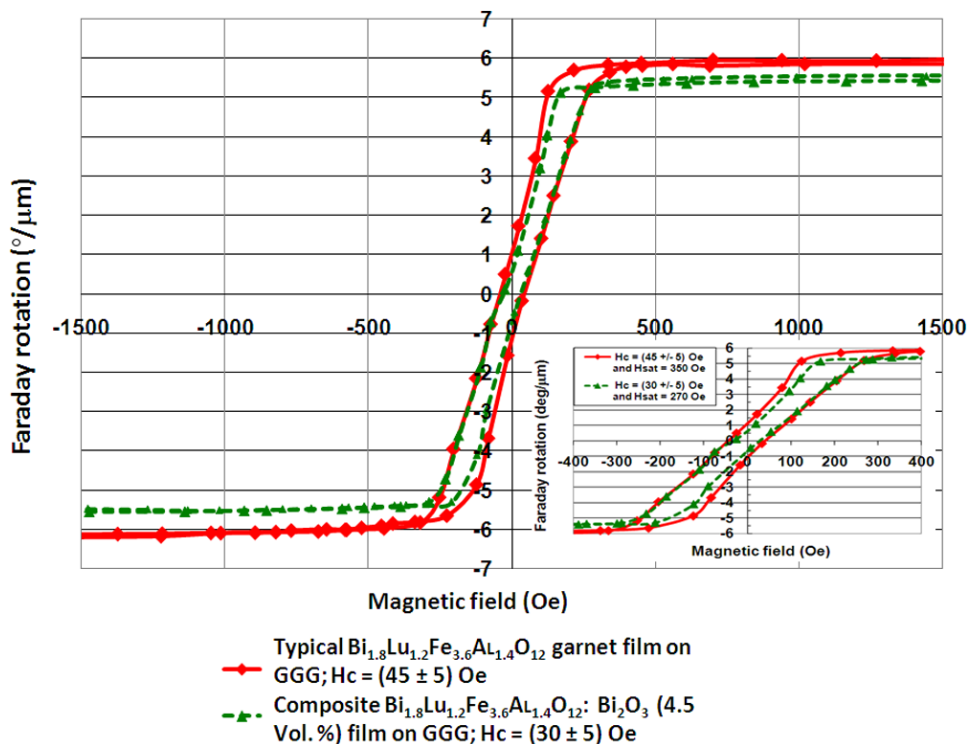
Figure 8. Results of magnetic hysteresis loop measurements obtained on single-layer quasi-in-plane magnetized films of $Bi_{1.8}Lu_{1.2}Fe_{3.6}Al_{1.4}O_{12}$ and nanocomposite-type films $Bi_{1.8}Lu_{1.2}Fe_{3.6}Al_{1.4}O_{12} : Bi_2O_3$. [17, 18].

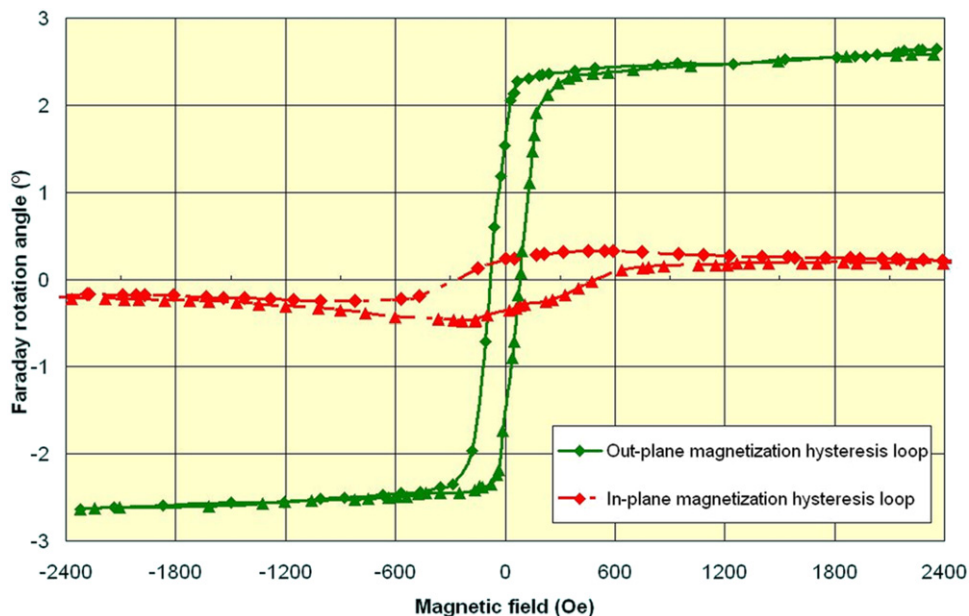**Figure 9.** Results of magnetic hysteresis loop measurements made with triple-layer film structures of composition $Bi_2Dy_1Fe_4Ga_1O_{12}$ (500 nm)–$Bi_{1.8}Lu_{1.2}Fe_{3.6}Al_{1.4}O_{12}$ (500 nm)–$Bi_2Dy_1Fe_4Ga_1O_{12}$ [19].

perpendicular to the structure's plane. Their hysteresis loops measured in the external magnetic fields applied in the direction perpendicular to the structure plane and also in the in-plane-directed fields are shown in figure 9.

In these triple-layer samples, the remanent magnetization was measured to be nearly 80% of the saturation magnetization. The structure investigated was far from being optimized perfectly because the intermediate layer was very thick. This resulted in 80% of remanent magnetization being

directed perpendicularly to the film's plane, which is partially related to the existence of a rather high coercive force in the material of the intermediate layer. We are now working on optimizing our experimental structures to attain an almost-rectangular hysteresis loop and a low coercive force of nearly 10 Oe. The experimental results obtained have shown that using the proposed exchange-coupled multilayers provided two orders of magnitude reduction in the typical switching field values required to drive pixels in MO spatial light modulators,

when compared with using existing single-layer materials. The results obtained can therefore provide a new solution for the practical realization of high-speed MO transparencies and switching devices.

4. Conclusion

The results of our theoretical and experimental study of all-garnet magnetic heterostructures have shown that it is possible to fabricate multilayer thin-film garnet structures that are very attractive for the creation of next-generation magnetic and magneto-optic materials. The theoretical framework suitable for predicting the parameters of multilayer structures based on Bi-substituted iron garnets has been developed, and the material design strategy suitable for the practical implementation of these structured MO material systems has been reported. The characterization results obtained with triple-layer all-garnet structures deposited using sequential RF-magnetron sputtering of two garnet materials possessing different anisotropy types confirm that it is possible to synthesize material systems with multiple magnetic and MO parameters optimized simultaneously. We demonstrated a new material system possessing a combination of high specific Faraday rotation, a nearly rectangular magnetic hysteresis loop and low coercivity.

Acknowledgments

References

[1] Paroli P 1984 Magneto-optical devices based on garnet films *Thin Solid Films* **114** 187–219

[2] Zvezdin A K and Kotov V A 1997 *Modern Magnetooptics and Magnetooptical Materials* (Bristol: Institute of Physics Publishing)

[3] http://www.bnonlinear.com/index.php sighted in April 2012

[4] Spain R J and Fuller H W 1966 Stripe domain in thin magnetic films and their application to magnet-optical displays *J. Appl. Phys.* **37** 953–9

[5] Almasi G S 1971 Magneto-optic bubble domain devices *IEEE Trans. Magn.* **7** 370–3

[6] Lacklison D E, Scott G B, Giles A D, Klarke J A, Pearson R F and Page J L 1977 *IEEE Trans. Magn.* **13** 93–981

[7] Hansen P, Tolksdorf W and Witter K 1984 Recent advance of bismuth garnet materials research for bubble and magneto-optical applications *IEEE Trans. Magn.* **20** 1099–104

[8] Okuda T, Katayama T, Kobayashi H and Satoh K 1990 Magnetic properties of $Bi_3Fe_5O_{12}$ garnet *J. Appl. Phys.* **67** 4944–6

[9] Kahl S and Grishin A M 2003 Pulsed laser deposition of $Y_3Fe_5O_{12}$ and $Bi_3Fe_5O_{12}$ films on garnet substrates *J. Appl. Phys.* **93** 6945–7

[10] Vasiliev M, Nur-E-Alam M, Kotov V A, Alameh K E, Belotelov V I, Burkov V I and Zvezdin A K 2009 RF-magnetron sputtered $(BiDy)_3(FeGa)_5O_{12} : Bi_2O_3$ composite garnet-oxide materials possessing record magneto-optic quality in the visible spectral region *Opt. Express* **17** 19519

[11] Vasiliev M, Nur-E-Alam M, Alameh K, Premchander P, Lee Y T, Kotov V A and Lee Y P 2011 Annealing behavior and crystal structure of RF-sputtered Bi-substituted dysprosium iron-garnet films having excess co-sputtered Bi-oxide content *J. Phys. D: Appl. Phys.* **44** 075002

[12] Nur-E-Alam M, Vasiliev M, Kotov V A and Alameh K 2011 Highly Bi-substituted, record-performance magneto-optic garnet materials with low coercivity for applications in integrated optics, photonic crystals, imaging and sensing *Opt. Mater. Express* **1** 413–27

[13] Nakagawa K, Kurashina S and Itoh A 1994 Uniaxial anisotropy of double-layered garnet films and magneto-optical recording characteristics *J. Appl. Phys.* **75** 7096–8

[14] Harvey W A, Nelson G L, Tolman C H and Torok E J 1982 Exchange coupled garnet films *IEEE Trans. Magn.* **18** 1340–2

[15] Ramesh R, Simion B M and Thomas G 1997 Epitaxial magnetic garnet heterostructures *J. Phys. IV France 7, Colloque C1, Supplement au Journal de Physique III de mar C1-695*

[16] Zvezdin A K, Ziubin V V and Popkov A F 1988 Quasi-statical vertical remagnetization of two-layer ferromagnetics *Russ. Microelectron. (in Russian)* **17** 165–7

[17] Nur-E-Alam M, Vasiliev M, Alameh K and Kotov V A 2011 Synthesis of high-performance magnetic garnet materials and garnet-bismuth oxide nanocomposites using physical vapor deposition followed by high-temperature crystallization *Pure Appl. Chem.* **83** 1971–80

[18] Nur-E-Alam M, Vasiliev M, Alameh K and Kotov V A 2011 Physical properties and behaviour of highly Bi-substituted magneto-optic garnets for applications in integrated optics and photonics *Adv. Opt. Technol.* **2011** 1–7

[19] Nur-E-Alam M, Vasiliev M, Alameh K and Kotov V A 2011 Garnet multilayer thin film structure with magnetostatically-altered and improved magnetic properties prepared by RF magnetron sputtering *Proc. 8th Int. Conf. on High-Capacity Optical Networks and Emerging Technologies (Riyadh, Kingdom of Saudi Arabia, 19–21 December 2011)* paper HS4B-4